John R. Hardy Papers

Research Papers in Physics and Astronomy

8-15-1971

Application of the Method of Lattice Statics to Vacancies in Aluminum

Larry Boyer
University of Nebraska - Lincoln

John R. Hardy
University of Nebraska - Lincoln

Application of the Method of Lattice Statics to Vacancies in Aluminum[†]

Larry L. Boyer[*]

Behlen Laboratory of Physics, University of Nebraska, Lincoln, Nebraska 68508

and

John R. Hardy

Lawrence Radiation Laboratory, University of California, Livermore, California 94550

In this paper the method of lattice statics is applied to the calculation of the atomic displacements about a vacancy in aluminum using a fifth-neighbor force-constant model for the dynamical matrix and the vacancy-host lattice interaction. The strain-field interaction energy between two vacancies is similarly calculated. The main object of this work is to demonstrate the important modifications of earlier results, obtained for a first- and second-neighbor force-constant model, when one uses the fifth-neighbor model designed to give a significantly better fit to the measured phonon dispersion curves. In particular it is demonstrated that the displacements about the vacancy continue to deviate strongly from the asymptotic elastic-continuum values out much farther from the defect than is the case for the first- and second-neighbor model.

I. INTRODUCTION

In this paper, using the method of lattice statics, we extend the calculations of Bullough and Hardy[1] for the displacement field about a vacancy in aluminum to include third-, fourth-, and fifth-nearest-neighbor interactions. As we shall see, by extending the range of the interatomic forces we correspondingly introduce long-range effects into the displacement field.

We assume that total crystal energy can be written as a sum of effective pairwise interactions between the ions and a volume-dependent contribution from the electron gas. This assumption is based on the pseudopotential theory of metals, in which the atoms are separated into ion cores and a "gas" of quasifree conduction electrons. Harrison[2] shows explicitly that the total energy contains a volume-dependent term and an effective pairwise central interaction between ion cores. We denote this by the interatomic potential $\Psi(r)$ (r being the appropriate spacing).

For a crystal with total potential energy resulting *entirely* from central pairwise interactions, the Cauchy relations must hold. For cubic crystals, this means that $C_{12} = C_{44}$, which are not equal for most cubic metals (including aluminum) because of the volume-dependent contribution to the total energy of the crystal. In other words, the crystal is required to be stable only under the *combined* influences of the central pairwise potentials and the volume-dependent part of the energy. Thus, the Cauchy relations are violated.

We make two approximations: First, we assume that the interatomic potential is of reasonably short range and is essentially zero for atoms farther apart than fifth-nearest neighbors. (Shyu and Gaspari[3] have shown that this is a reasonable assumption for all alkali metals except lithium; in this paper we show that a fifth-neighbor model for aluminum provides a good over-all fit to neutron diffraction data.) Second, we expand the energy of the crystal to the harmonic approximation. Our calculations *suggest* that this is reasonable since the displacements we obtain are typically less than a few percent of interatomic spacing. However, this restriction can be removed when we have a reliable interatomic potential which is valid for all values of r.

The method of lattice statics, originally introduced by Kanzaki,[4] involves writing the displacement field about a defect as a Fourier sum, where the coefficients are obtained by Fourier transforming the equilibrium equations. The displacements calculated, with this Fourier sum, are exact, within the harmonic approximation and the assumption of periodic boundary conditions, and in no way depend on fitting the displacements of atoms "far" from the defect to certain assumed values. That is, this method allows for the simultaneous relaxation of all the atoms, and is therefore superior to direct space calculations (see, for example, Ref. 3) which assume that atoms outside a certain region (region I) centered on the defect are either held fixed or forced to relax to positions determined by elasticity theory. The major difficulty with such calculations is that one does not know *a priori* how large to make this region.

Let us take the region to be spherical with radius R_0 and define it as that region in which the strain field is not adequately described by continuum elasticity theory. The displacements calculated in

TABLE I. Force constants α_i for both isotropic and anisotropic aluminum together with coefficients $\underline{A}_{ij}$ and β_j in Eq. (6)—units of α_i and β_j are 10^4 dyn/cm.

j $\backslash$ i	1	2	3	4	5	6	7	8	9	10	α_j Aniso-tropic	α_j Iso-tropic	β_j Aniso-tropic	β_j Iso-tropic
1	0.5	−0.5	2.0	−2.0	3.0	−3.0	2.0	−2.0	14.6	−14.6	4.3232	4.3008	3.2392	3.6441
2	0.5	1.5	0.0	2.0	6.0	9.0	2.0	6.0	1.8	18.2	−0.3403	−0.3627	1.1337	1.1337
3	1.0	−1.0	0.0	0.0	6.0	−6.0	4.0	−4.0	3.6	−3.6	0.1919	0.3268	3.6447	3.6447
4	4.0	4.0	0.0	0.0	2.6667	13.333	0.0	0.0	8.0	8.0	0.0217	−0.0457	16.0	16.0
5	2.0	6.0	0.0	0.0	6.6667	9.333	0.0	0.0	4.0	12.0	−0.0779	−0.0151	6.072	6.072
6	1.0	5.0	2.0	4.0	4.6667	7.3333	0.0	0.0	5.2	6.8	−0.0118	0.0510	2.9	2.9
7	4.0	2.0	2.0	4.0	2.6667	9.3333	0.0	0.0	1.6	10.4	−0.1533	−0.1196	16.7	16.7
8	2.707	5.121	1.0	1.0	2.1143	7.8857	3.0	3.0	4.4688	9.5312	0.0778	0.1116	9.856	9.856
9	1.707	6.121	1.0	1.0	5.2191	4.7809	1.0	5.0	3.2688	10.731	0.0692	0.0175	5.3486	5.3486
10	2.10	4.0	0.0	4.0	4.0	8.0	4.0	4.0	4.0	8.0	−0.0149	−0.0666	6.821	6.821

Ref. 1, with a second-neighbor central-force model, indicate that, for a vacancy in aluminum, $R_0 \cong 6a$, where $\sqrt{2}\, a$ is the first-nearest-neighbor separation. For the more realistic fifth-neighbor model our results set a lower limit for R_0 of about $25a$. There are approximately 30 000 atoms in a region this size. Clearly, a direct space calculation which allows for the simultaneous relaxation of all atoms within a region I of radius $\cong 25a$ is for practical purposes impossible.

In Sec. II we give a resume of the method of lattice statics with particular emphasis on the assumption of periodic boundary conditions. We prefer to call this the superlattice assumption and will refer to it as such in what follows. In Sec. III we list the formulas pertinent to our problem and discuss in some detail the procedure used to obtain the constants in these equations. Results are listed and discussed in Sec. IV.

II. METHOD OF LATTICE STATICS

Since a detailed account of the method of lattice statics has recently been given by Flocken and Hardy,[5] we will present only the basic assumptions and resultant formulas along with a brief discussion of the dependence of the strain field on the volume of periodicity.

Consider an infinite monatomic[6] lattice with identical point defects regularly spaced to form a superlattice of defects having the same structure as the host lattice and containing N lattice points per defect. By symmetry the strain field due to the superlattice is periodic over a Wigner-Seitz volume (supercell) containing N lattice points and one de-

TABLE II. Comparison of calculated phonon frequencies with corresponding experimental values.

Direction of $\vec{q}$	T or E^b	$m\omega^2$ for $\dfrac{\vec{q}}{\vec{q}\ \text{(zone boundary)}^a}$						
		0.4	0.5	0.6	0.7	0.8	0.9	1.0
⟨100⟩	E	1.82	2.74	3.69	4.48	5.21	5.83	6.07
	T	2.07	3.05	4.04	4.90	5.55	5.94	6.07
⟨100⟩	E	6.15	8.42	10.50	12.34	14.05	15.45	16.00
	T	5.47	7.63	9.87	12.09	14.07	15.49	16.00
⟨111⟩	E	1.11	1.65	2.04	2.42	2.55	2.55	2.55
	T	1.18	1.65	2.07	2.43	2.69	2.85	2.90
⟨111⟩	E	4.69	7.02	10.08	13.23	16.30	17.34	16.30
	T	5.30	7.83	10.47	12.93	14.94	16.26	16.72
⟨110⟩	E	2.35	3.68	5.45	7.51	9.49	11.31	12.95
	T	2.43	3.82	5.54	7.49	9.57	11.58	13.33
⟨110⟩	E	1.81	2.55	3.21	3.83	4.44	4.98	5.35
	T	1.48	2.04	2.66	2.34	4.07	4.77	5.35
⟨110⟩	E	6.87	9.43	11.72	13.05	13.10	11.91	9.86
	T	6.89	9.40	11.34	12.37	12.35	11.40	9.86

$^a m\omega^2$ is in units of 10^4 dyn/cm; m = atomic mass. ^{b}T denotes theoretical; E experimental.
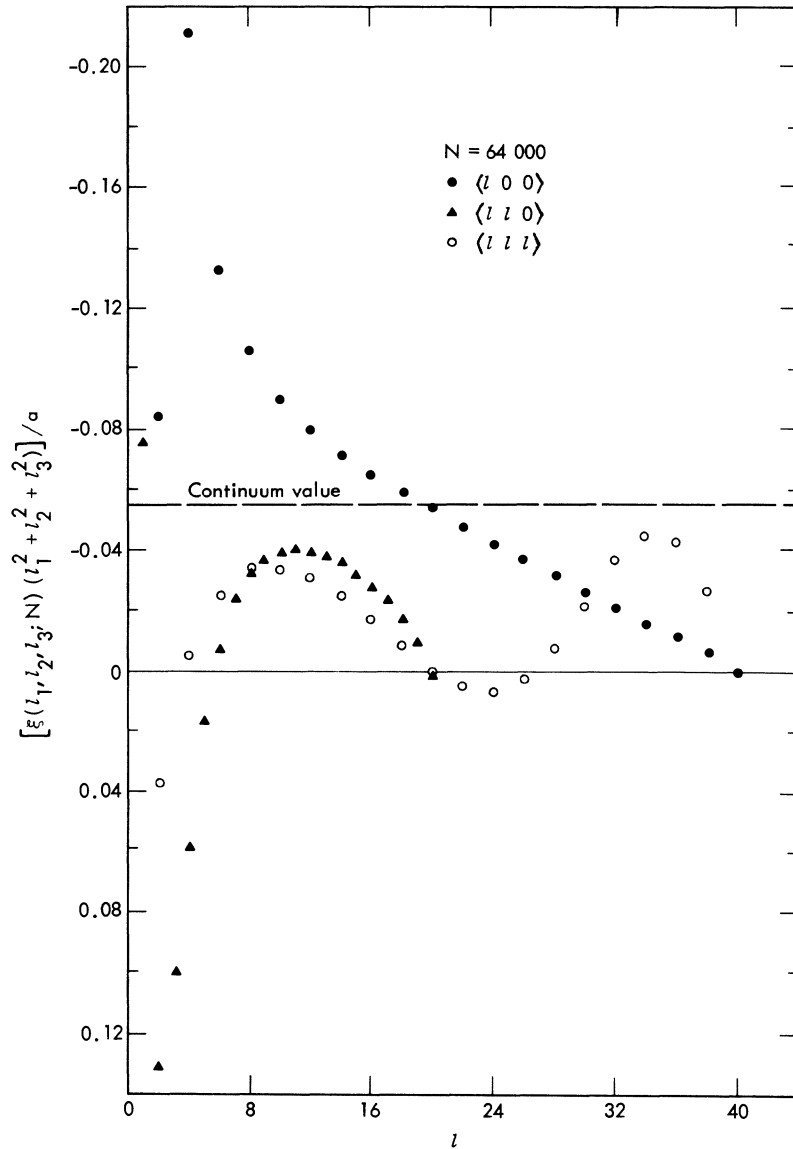
FIG. 1. $[\vec{\xi}\,\vec{1};N) \times (l_1{}^2 + l_2{}^2 + l_3{}^2)]/a$ vs l for $\vec{r}(\vec{l})$ along the $\langle 100 \rangle$, $\langle 110 \rangle$, and $\langle 111 \rangle$ directions using the P method with 64 000 sample points (i.e., N = 64 000).

TABLE III.   Comparison of displacements $-[\xi(l,\ l,\ l) \times 3l^2]/a$ at selected points obtained using P and Q methods.

| | Displacements | | | | | | | |
| | P method | | | | Q method | | | |
Lattice points	8000 samples	64 000 samples	512 000 samples	4 096 000 samples	4 000 samples	32 000 samples	55 296 samples	256 000 samples
(4, 4, 4)	0.001623	0.005428	0.005972		0.006288	0.006046	0.006046	0.006046
(8, 8, 8)	0.009936	0.032531	0.036824		0.036356	0.037420	0.037421	0.037421
(12, 12, 12)		0.030763	0.044483		−1.919646	0.046502	0.046507	0.046509
(16, 16, 16)		0.016820	0.045137	0.049360	8.401566	0.049922	0.049949	0.049957
(20, 20, 20)		0.0	0.042198	0.050413	1.004831	0.050872	0.051568	0.051584
(24, 24, 24)			0.036494	0.050443	−0.137893	−2.605500	0.052298	0.052473
(28, 28, 28)			0.028462				−0.711894	0.053010
(32, 32, 32)			0.018795					0.053357
(36, 36, 36)			0.008714					0.053545
(40, 40, 40)			0.0					0.053763
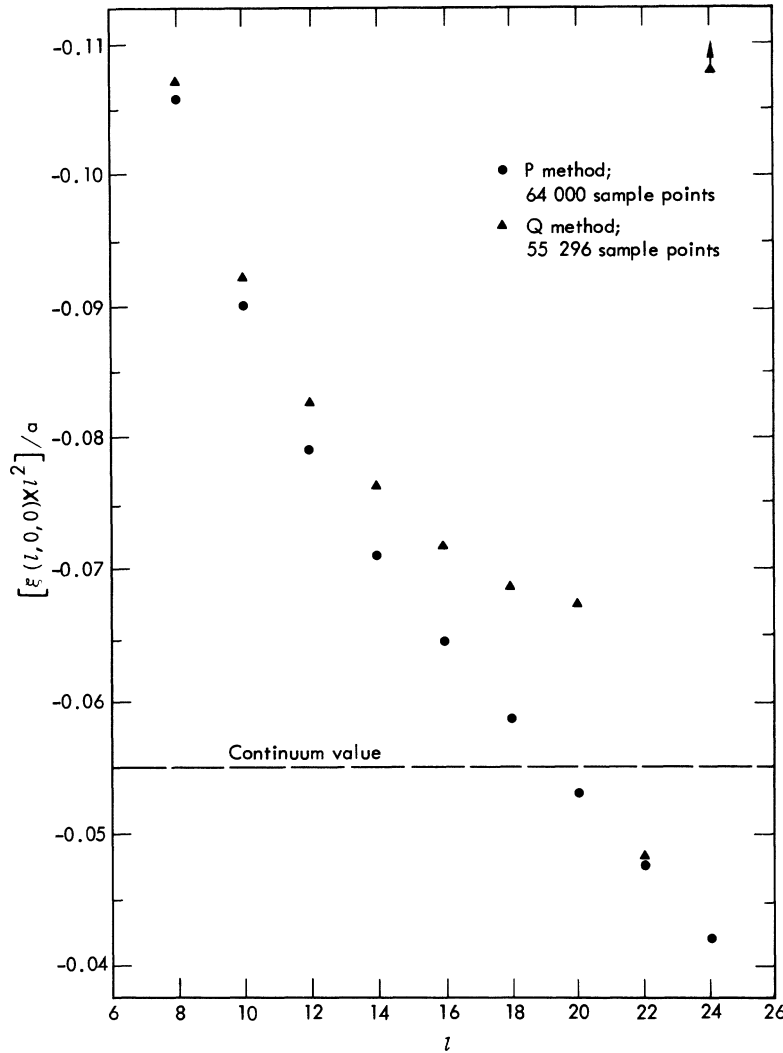
FIG. 2. $[\vec{\xi}(l, 0, 0) \times l^2]/a$ vs l using both P and Q methods with comparable numbers of sample points ($\vec{q}$ vectors) in the first B. Z.

fect. This hypothetical periodicity permits a Fourier transformation of the $3N$ equilibrium equations which leads to the strain field given by a summation over the N wave vectors (reciprocal-superlattice vectors) of the first Brillouin zone (B. Z.); namely,[7]

$$\vec{\xi}(\vec{l};N) = (1/N) \sum_{\vec{q}} [\overline{V}(\vec{q})]^{-1} \vec{F}(\vec{q}) e^{i\vec{q}\cdot\vec{r}(\vec{l})} . \quad (1)$$

The term $\vec{\xi}(\vec{l};N)$ is the displacement of the $\vec{l}$th atom for its perfect lattice position at $\vec{r}(\vec{l})$ due to a superlattice of size N. The term $[\overline{V}(\vec{q})]^{-1}$ is the inverse of the dynamical matrix for wave vector $\vec{q}$ exclusive of the inverse mass factor. The term $\vec{F}(\vec{q})$ is defined by

$$\vec{F}(\vec{q}) = \sum_{\vec{l}} \vec{f}(\vec{l}) e^{i\vec{q}\cdot\vec{r}(\vec{l})} , \quad (2)$$

where $\vec{f}(\vec{l})$ is the force on the $\vec{l}$th atom in its displaced position due to the defect at the origin.

Similar arguments have led Hardy and Bullough[8] to the following expression for the interaction energy of a defect at the origin with a second defect at $\vec{r}(\vec{l})$:

$$E(\vec{l};N) = (-1/N) \sum_{\vec{q}} \bar{\vec{F}}(\vec{q}) [\overline{V}(\vec{q})]^{-1} \vec{F}(\vec{q}) \cos[\vec{q}\cdot\vec{r}(\vec{l})] . \quad (3)$$

The summation over $\vec{q}$ in Eqs. (1) and (3) includes all the distinct wave vectors in the first B. Z. If we let $q_i = (n_i/M) \times (\pi/a)$ (where $M^3 = N$), the allowed wave vectors for the fcc lattice are those for which n_1, n_2, and n_3 are either all odd or all even integers with $n_1 + n_2 + n_3 \leq \frac{1}{2} 3M$.

Considering only the three symmetry directions, boundary conditions require zero displacements for points $(\frac{1}{2}M, \frac{1}{2}M, 0)$, $(M, 0, 0)$, and (M, M, M), since these are points of inversion symmetry for the superlattice. Although the point $(\frac{1}{2}M, \frac{1}{2}M, \frac{1}{2}M)$ is not a point of inversion symmetry, it is the center
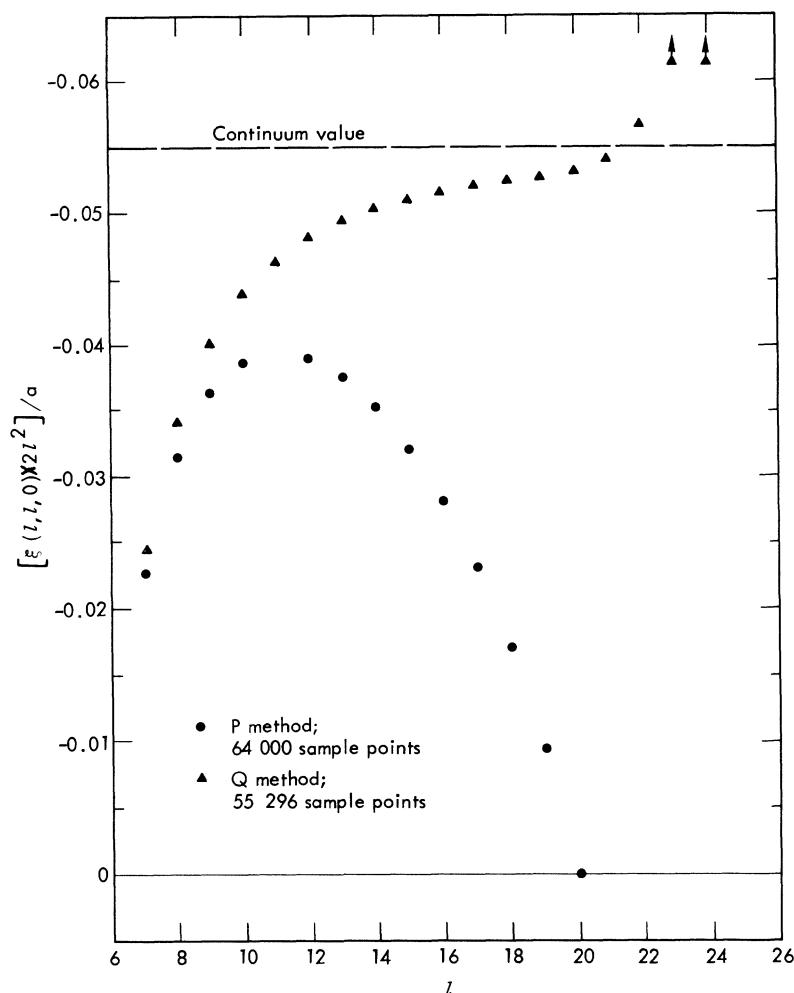
FIG. 3. $[\vec{\xi}(l,\,l,\,0)\times 2l^2]/a$ vs l using both P and Q methods with comparable numbers of sample points ($\vec{q}$ vectors) in the first B. Z.

of the tetrahedron formed by the vacant sites at $(0,0,0)$, $(M,M,0)$, $(M,0,M)$, and $(0,M,M)$. Therefore, the displacement of the atom at this point is also forced to zero. These symmetry requirements are somewhat troublesome since we want to obtain the displacement field of an *isolated* vacancy. However, by using increased values for N, we can identify the effect of this imposed symmetry and estimate the displacements caused by an isolated vacancy.

The above sampling technique (which we call the P method) has been widely used since the advent of computers as the method for treating problems which require a summation over lattice vibrational modes. A recent example of lattice-statics calculations with this method is given by Flocken and Hardy.[5]

It was mentioned above that the method of lattice statics is exact within the harmonic approximation and the superlattice assumption. The superlattice assumption introduces the dependence of $\vec{\xi}$ and E on N. This is not a serious difficulty if the range

of the atom-atom and atom-defect forces is small compared to the size of the maximum attainable supercell.[9] For such problems, $\vec{\xi}(\vec{l};N_{max})$ and $[E(\vec{l};N_{max})]$ are good approximations to $\vec{\xi}(\vec{l};\infty)$ and $[E(\vec{l};\infty)]$ for all $\vec{l}$ such that $|\vec{r}(\vec{l})| < R_0$. For $|\vec{r}(\vec{l})| > R_0$, i.e., where the method of lattice statics becomes continuum theory, $\vec{\xi}(\vec{l};\infty)$ and $E(\vec{l};\infty)$ are best calculated by a technique introduced by Kanzaki[4] and used by Hardy and Bullough[1,8] and Flocken,[10] which converts the summation over $\vec{q}$ to a single integration over the azimthual angle about the direction in $\vec{q}$ space along $\vec{r}(\vec{l})$. We have found that increasing the range of the interatomic forces to include fifth-neighbor interactions increases R_0 so much that the symmetry requirements of the P method become very marked (Fig. 1).

An alternate approach is that of letting the volume of periodicity become infinite. Thus,

$$(1/N)\sum_{\vec{q}} \to [v/(2\pi)^3]\int_{B.Z.} d\vec{q}\,, \qquad (4)$$

where v is the volume per atom and the integration is over the first B.Z. For most realistic problems, the integral must be performed numerically. In face, the above sampling technique may be considered as a numerical approximation to the integral.

Another method, the random-sampling technique used by Bullough and Hardy,[1] eliminates the problem of periodicity but is not very efficient for obtaining accurate numerical results. However, much more efficient numerical methods do exist for the approximation of single integrals and may be applied to this multiple integral. We might expect that this would be a very difficult problem because of the complex shape of the B.Z. Fortunately, this is not the case.

Note that

$$\int_{\text{B.Z.}} h(\vec{q})\, d\vec{q} = \tfrac{1}{2} \int_C h(\vec{q})\, d\vec{q} , \qquad (5)$$

where $h(\vec{q})$ is any function with the periodicity of the reciprocal lattice and C denotes the cube inscribing the first B.Z. Thus, in units where $a=1$, the displacements become

$$\vec{\xi}(\vec{l}; \infty) = [1/(2\pi)^3] \int_{-\pi}^{\pi} \int_{-\pi}^{\pi} \int_{-\pi}^{\pi} \overleftrightarrow{V}^{-1}(x,y,z) \vec{F}(x,y,z)$$

$$\times \exp[i(l_1 x + l_2 y + l_3 z)]\, dx\, dy\, dz , \qquad (6)$$

where $x=q_1 a$, $y=q_2 a$, and $z=q_3 a$. The constant limits on this integral permit it to be solved easily by the generalization to multiple integrals of conventional methods for the numerical integration of single integrals.

One of the most efficient methods is the Gaussian quadrature method.[11] If we use the Gaussian quadrature with n positive roots, $\vec{\xi}(\vec{l})$ is approximated by

$$\vec{\xi}(\vec{l}; \infty) \cong \tfrac{1}{8} \sum_{i,j,k} \overleftrightarrow{G}(x_i, x_j, x_k) W_i W_j W_k , \qquad (7)$$
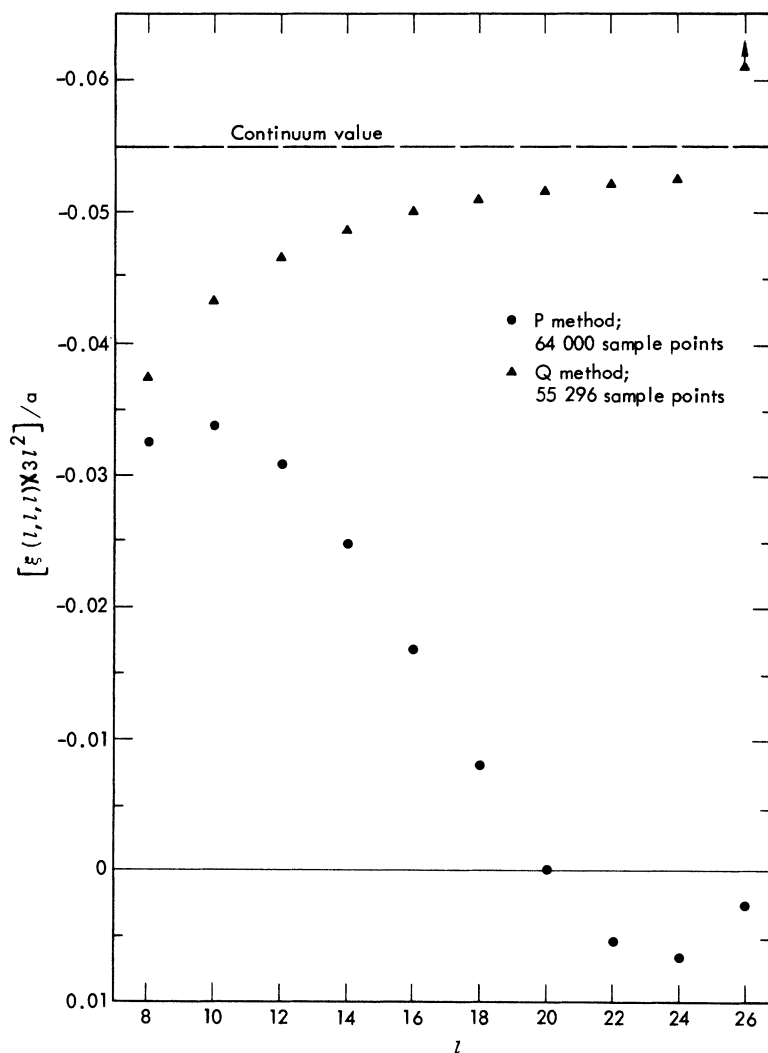

FIG. 4. $[\vec{\xi}(l, l, l) \times 3l^2]/a$ vs l using both P and Q methods with comparable numbers of sample points ($\vec{q}$ vectors) in first B. Z.

where i, j, and k are summed from $-n$ to n (excluding zero), and $\vec{G}$ is the integrand in Eq. (6). The x_i s π times the ith Gaussian abscissa and W_i is the ith Gaussian weight.

Note that we obtain a much denser sample of points in our integration volume near the corners of the cube than we do at the origin. As we also need a dense sample of points at the origin, because of the singularity in $\vec{V}^{-1}$ at the corners and the origin, we approximate $\vec{\xi}(\vec{l})$ by

$$\vec{\xi}(\vec{l}; \infty) = \tfrac{1}{8} \sum_{i,j,k} \vec{G}(x_i', x_j', x_k') W_i' W_j' W_k' \quad , \qquad (8)$$

where i, j, and k are now summed from $-2n$ to $2n$, $x_i' = (\tfrac{1}{2}\pi)(1 - x_i)$ and $W_i' = \tfrac{1}{2}W_i$ for $|i| \le n$, and $x_i' = (\tfrac{1}{2}\pi)(1 + x_{i-n})$ and $W_i' = \tfrac{1}{2}W_{i-n}$ for $|i| > n$.

This numerical integration method will be referred to as the Q method. For both the P and Q methods, we can shorten the calculations considerably by accounting for the symmetry of $\vec{G}$.

III. SPECIFIC FORMULAS

We wish to apply this method to the case of a vacancy in aluminum, a crystal which has the face-centered cubic structure. The aluminum atoms are positioned at sites: $\vec{r}(\vec{l}) = (l_1, l_2, l_3)a$, where $\vec{r}(\vec{l})$ is referred to the usual cubic axes with the origin at a vacancy of the superlattice. The l_1, l_2, and l_3 are integers such that $l_1 + l_2 + l_3$ is even and $a = 2.02$ Å. However, there are only $\tfrac{1}{48}N$ nonequivalent $\vec{r}(\vec{l})$ vectors because of the superlattice assumption and the fact that the cubic point group contains 48 symmetry operations.

Our model assumes that each atom interacts with its nth shell of nearest neighbors via a central potential $\Psi(r)$, where $\Psi(r)$ is constant for $n \ge 6$.

TABLE IV. Displacements about vacancy for lattice points with $l_1^2 + l_2^2 + l_3^2 \le 54$ together with corresponding interaction energies between pairs of vacancies at same separation (computed using the Q method with 55 296 sample points).

Lattice points (l_1, l_2, l_3)	Displacement components ξ_1/a	ξ_2/a	ξ_3/a	Interaction energies $E(\vec{l})$ eV
(1, 1, 0)	-0.01950	-0.01950	0.0	-0.07218
(2, 0, 0)	-0.02106	0.0	0.0	-0.04552
(2, 1, 1)	-0.00361	0.00375	0.00375	0.03055
(2, 2, 0)	0.01162	0.01162	0.0	-0.00035
(2, 2, 2)	0.00179	0.00179	0.00179	-0.00261
(3, 1, 0)	-0.02480	-0.00468	0.0	0.00261
(3, 2, 1)	0.00051	0.00096	0.00118	-0.01304
(3, 3, 0)	0.00422	0.00422	0.0	-0.01968
(3, 3, 2)	0.00060	0.00060	0.00045	-0.00170
(4, 0, 0)	-0.01333	0.0	0.0	0.03280
(4, 1, 1)	-0.00927	-0.00333	-0.00333	0.01504
(4, 2, 0)	-0.00600	-0.00382	0.0	0.00601
(4, 2, 2)	-0.00030	-0.00033	-0.00033	-0.00269
(4, 3, 1)	0.00032	0.00019	0.00014	0.00082
(4, 3, 3)	0.00008	0.00001	0.00001	-0.00200
(4, 4, 0)	0.00128	0.00128	0.0	0.01209
(4, 4, 2)	0.00010	0.00010	0.00011	0.00046
(4, 4, 4)	-0.00007	-0.00007	-0.00007	-0.00133
(5, 1, 0)	-0.00571	-0.00161	0.0	0.00069
(5, 2, 1)	-0.00367	-0.00194	-0.00010	-0.01006
(5, 3, 0)	-0.00199	-0.00151	0.0	-0.00919
(5, 3, 2)	-0.00041	-0.00043	-0.00028	-0.00117
(5, 4, 1)	0.00000	-0.00011	0.00002	0.00258
(5, 4, 3)	-0.00010	-0.00015	-0.00010	-0.00053
(5, 5, 0)	0.00024	0.00024	0.0	0.00584
(5, 5, 2)	-0.00010	-0.00010	-0.00002	0.00094
(6, 0, 0)	-0.00368	0.0	0.0	0.02056
(6, 1, 1)	-0.00322	-0.00071	-0.00071	0.00878
(6, 2, 0)	-0.00278	-0.00123	0.0	0.00201
(6, 2, 2)	-0.00194	-0.00089	-0.00089	-0.00437
(6, 3, 1)	-0.00160	-0.00108	-0.00039	-0.00464
(6, 3, 3)	-0.00047	-0.00036	-0.00036	-0.00088
(6, 4, 0)	-0.00082	-0.00074	0.0	-0.00285
(7, 1, 0)	-0.00227	-0.00039	0.0	0.00584

The elements of the dynamical matrix for this model are

$$V_{11}(q_1, q_2, q_3) = 2\alpha_1 + 4\alpha_2 + \alpha_3 + 2\alpha_4 + 4\alpha_5 + 8\alpha_6 + 2\alpha_7 + 4\alpha_8 + 4\alpha_9 + 8\alpha_{10} - (\alpha_1 + \alpha_2)\cos q_1 a(\cos q_2 a + \cos q_3 a)$$

$$- 2\alpha_2 \cos q_2 a \cos q_3 a - \alpha_3 \cos 2q_1 a - \alpha_4(\cos 2q_2 a + \cos 2q_3 a) - (\tfrac{2}{3}\alpha_5 + \tfrac{10}{3}\alpha_6)\cos q_1 a(\cos q_2 a \cos 2q_3 a$$

$$+ \cos 2q_2 a \cos q_3 a) - (\tfrac{8}{3}\alpha_5 + \tfrac{4}{3}\alpha_6)\cos 2q_1 a \cos q_2 a \cos q_3 a - (\alpha_7 + \alpha_8)\cos 2q_1 a(\cos 2q_2 a + \cos 2q_3 a)$$

$$- 2\alpha_8 \cos 2q_2 a \cos 2q_3 a - (\tfrac{1}{5}\alpha_9 + \tfrac{1}{5}9\alpha_{10})\cos q_1 a(\cos 3q_2 + \cos 3q_3 a)$$

$$- (\tfrac{1}{5}9\alpha_9 + \tfrac{1}{5}\alpha_{10})\cos 3q_1 a(\cos q_2 a + \cos q_3 a) - 2\alpha_{10}(\cos q_2 a \cos 3q_3 a + \cos 3q_2 a \cos q_3 a) \quad ,$$

$$V_{12}(q_1, q_2, q_3) = (\alpha_1 - \alpha_2)\sin q_1 a \sin q_2 a + (\tfrac{2}{3})(\alpha_5 - \alpha_6)(\sin q_1 a \sin q_2 a \cos 2q_3 a + 2\sin q_1 a \sin q_2 a \cos q_3 a$$

$$+ 2\sin 2q_1 a \sin q_2 a \cos q_3 a) + (\alpha_7 - \alpha_8)\sin 2q_1 a \sin 2q_2 a + (\tfrac{3}{5})(\alpha_9 - \alpha_{10})(\sin q_1 a \sin 3q_2 a + \sin 3q_1 a \sin q_2 a);$$

$$V_{22}(q_1, q_2, q_3) = V_{11}(q_2, q_3, q_1) \ ,$$

$$V_{33}(q_1, q_2, q_3) = V_{11}(q_3, q_1, q_2) \ ,$$

$$V_{13}(q_1, q_2, q_3) = V_{12}(q_3, q_1, q_2) \ ,$$

$$V_{23}(q_1, q_2, q_3) = V_{12}(q_2, q_3, q_1) \ ,$$

$$V_{23} = V_{32}, \quad V_{12} = V_{21}, \quad V_{13} = V_{31} \ , \tag{9}$$

where

$$\alpha_{2n-1} = 2\left(\frac{\partial^2 \Psi(r)}{\partial r^2}\right)_{r(n)} \ , \quad \alpha_{2n} = 2\left(\frac{1}{r}\frac{\partial \Psi(r)}{\partial r}\right)_{r(n)} \ , \tag{10}$$

and $\sqrt{2}a$ is the first-nearest-neighbor separation. The subscripts on the derivatives indicate the value of r which at the derivatives are evaluated.

The numerical values for the α's were obtained by solving a set of 10 linear equations:

$$\sum_{i=1}^{10} A_{ij}\alpha_i = \beta_j \ ; \quad j = 1, 2, \ldots, 10 \ . \tag{11}$$

The coefficient matrix $\underline{A}$ is determined from the dynamical matrix by inserting particular values for $\vec{q}$. Three equations can be obtained in the $\vec{q} \to 0$ limit, where the corresponding β_j are functions of the elastic constants, determined by comparing $\overline{\overline{V}}(\vec{q})$ with the dynamical matrix of elastic theory. Any number of equations can be obtained for $\vec{q} > 0$ with the corresponding β_j being eigenvalues of $\overline{\overline{V}}(\vec{q})$ taken from experimental phonon dispersion curves.

Several sets of force constants were determined by using different sets of 10 equations. The reproducibility of the experimental phonon dispersion curves was checked for each set of α's. The 10 equations (shown in Table I along with the solutions, α_i) chosen as giving the best over-all fit were: the three $\vec{q} \to 0$ equations ($j = 1, 2, 3$); the two $\langle 100 \rangle$

zone-boundary equations ($j = 4, 5$); the two $\langle 111 \rangle$ zone-boundary equations ($j = 6, 7$); the longitudinal $\langle 110 \rangle$ zone-boundary equation ($j = 8$); the transverse $\langle 110 \rangle$ zone-boundary equation for modes with polarization along the $\langle 1 - 10 \rangle$ direction ($j = 9$); and the transverse $\vec{q} = (\pi/2a)(1, 1, 0)$ mode with polarization along the $\langle 001 \rangle$ direction ($j = 10$). The experimental values for $\vec{q}$ along the $\langle 100 \rangle$ and $\langle 110 \rangle$ directions are those of Yarnell, Warren, and Koenig.[12] For $\vec{q}$ along the $\langle 111 \rangle$ direction, Walker's results[13] were used. The elastic constants C_{11}, C_{12}, and C_{44} used were, respectively, 1.08×10^{12}, 0.62×10^{12}, and 0.28×10^{12} dyn/cm^2.

The ability of the force constants in Table I to reproduce the experimental dispersion curves is demonstrated in Table II.

We were also interested in obtaining force constants which would give us elastic isotropy, since the relation $\vec{\xi}(\vec{r}) \propto \vec{r}/r^3$, valid for an isotropic elastic medium, is useful for comparison with the results of lattice statics. To obtain isotropic force constants (also shown in Table I), we merely replaced C_{11} with $C_{12} + 2C_{44}$ in Eq. (11).

From symmetry considerations alone the forces on the first-, second-, and fourth-nearest neighbors due to the vacancy are radial. Since the force constants for third and fifth neighbors are relatively small, we assume the forces on these neighbors to be radial also. With this assumption the Fourier transformed forces become

$$F_1(\vec{q}) = i\{2\sqrt{2}f_1 \sin q_1 a(\cos q_2 a + \cos q_3 a) + 2f_2 \sin 2q_1 a + \tfrac{4}{3}\sqrt{6}f_3 [2\sin 2q_1 a \cos q_2 a \cos q_3 a + \sin q_1 a(\cos 2q_2 a \cos q_3 a$$

$$+ \cos q_2 a \cos 2q_3 a)] + 2\sqrt{2}f_4 \sin 2q_1 a(\cos 2q_2 a + \cos 2q_3 a) + \tfrac{2}{5}\sqrt{10}f_5 [3\sin 3q_1 a(\cos q_2 a + \cos q_3 a)$$

$$+ \sin q_1 a(\cos 3q_2 a + \cos 3q_3 a)]\} \ ;$$

$$F_2(q_1, q_2, q_3) = F_1(q_2, q_3, q_1)$$

and

$$F_3(q_1, q_2, q_3) = F_1(q_3, q_1, q_2) \ ,$$

where f_n is the force on the nth neighbor $= [\partial \Psi(r)/$

$\partial r]_{r(n)}$.

The numerical values of the f_n's for isotropic aluminum were obtained by the same method as that used by Bullough and Hardy,[1] following Kanzaki,[4] with the exception that there are five unknown forces to be determined:

n	1	2	3	4	5
f_n/a(dyn/cm)	-3156.8	-491.8	625.4	1568.3	-1054.9

where f_n is positive for outward radial forces.

IV. RESULTS

The required summations in Eqs. (1), (3), and (8) were done for the isotropic aluminum model discussed in Sec. III using an IBM 360/65 computer.

In Figs. 1–4, we show the displacements for atoms along each of the three symmetry directions. These are intended to show the general function dependence of $\vec{\xi}$ on $\vec{l}$ and N. The symmetry of the superlattice is exhibited in Fig. 1 where $[\vec{\xi}(l_1, l_2, l_3; 64\,000)(l_1^2 + l_2^2 + l_3^2)]/a$ is plotted for the three symmetry directions. Since continuum theory predicts a $1/r^2$ dependence for $\vec{\xi}(\vec{r})$, the continuum result for such a plot is a horizontal line. The continuum value -0.0550 is easily calculated from the forces $\vec{f}(\vec{l})$ as shown by Hardy.[14] A continuum value of -0.0542 was obtained by Bullough and Hardy[1] with their second-neighbor model. Moving in the direction of $+\vec{l}$ (Fig. 1), we see the results of the lattice statics tending toward the continuum value before being forced to zero at $(40, 0, 0)$, $(40, 40, 40)$, $(20, 20, 0)$, and $(20, 20, 20)$ by the symmetry of the superlattice.

In Figs. 2–4, the P and Q methods are compared for atoms along the $\langle 100 \rangle$, $\langle 110 \rangle$, and $\langle 111 \rangle$ directions, respectively. The number of sample points used were 64 000 and 55 296, respectively, for the P and Q methods. These plots are magnifications of the regions in Fig. 1 where the superlattice assumption has drastic effects on the P-method calculations.

From these figures it is clear that, even though the number of sample points used in the Q calculations was less than that used in the P calculations, the Q results maintain accuracy over a much larger region than do the P results. In fact, we can definitely see that the lattice-statics displacements approach the elastic limit before the results of the Q calculations abruptly become absurd. This abruptness with which the Q results obviously become ridiculous aids in determining the region of validity of these calculations.[15]

As a further check on the computational accuracy of these two methods, we have compared $\vec{\xi}(l, l, l; \infty) \times 3l^2$ using a variety of sample point densities.

These results (Table III) also indicate that the Q method is much more efficient than is the P method.

For completeness, we show in Table IV the displacements and interaction energies for lattice points with $l_1^2 + l_2^2 + l_3^2 \leq 54$. These results are for isotropic aluminum using the Q method with 55 296 sample points.

Finally, this work using the fifth-neighbor model demonstrates important modifications of earlier results[1] obtained for a second-neighbor force-constant model. Specifically, the displacements continue to deviate strongly from the asymptotic values much farther from the defect than is the case for the second-neighbor model. The second-neighbor calculations indicate that, for isotropic aluminum, $\vec{\xi}(\vec{l}) \times (l_1^2 + l_2^2 + l_3^2)$ is within about 10% of the continuum value for atoms farther than approximately $6a$ from the defect. For the fifth-neighbor model the 10% discrepancy is maintained for atoms at least as far as $20a$ from the vacancy. It is these long-range effects that render any semidiscrete calculations impractical.

Because of the forced elastic isotropy and the possible inadequacy of the fifth-neighbor central-force model, the results presented here should not be expected to describe exactly the distortions about a vacancy in a real aluminum crystal. Indeed, we found that the force constants α_i were rather sensitive to the particular set of experimental values β_i used in Eq. (11), indicating that the model needs improvement.

However, these limitations do not affect the main point of this work; namely, that an extension of the range of the interatomic forces may correspondingly increase the region in which the predictions of elastic theory are inadequate. The point is that our results are *exact* for the set of force constants α [cf. Eq. (10)] we have used and the resultant displacements are directly comparable with those in an isotropic continuum having the same elastic constants. Furthermore, the assumption of radial third- and fifth-neighbor forces is good since relaxation changes both f_3 and f_5 by approximately 0.2% as compared with their zero-order counterparts. Since these last forces are purely radial, it follows that f_3 and f_5 are also radial to a very good approximation.

[1] R. Bullough and J. R. Hardy, Phil. Mag. 17, 833 (1968).

[2] W. A. Harrison, *Pseudopotentials in the Theory of Metals* (Benjamin, New York, 1966), p. 43.

[3] W. M. Shyu and G. D. Gaspari, Phys. Rev. 163, 667 (1967).

[4] H. Kanzaki, J. Phys. Chem. Solids 2, 24 (1957).

[5] J. W. Flocken and J. R. Hardy, Phys. Rev. 175, 919 (1968); and 177, 1054 (1969).

[6] The generalization to polyatomic crystals is straightforward.

[7] This expression for the displacements was obtained by minimizing the energy of the crystal at constant volume. Strictly speaking, one must also minimize the energy with respect to a uniform lattice dilatation. However, Hardy (Ref. 14) has shown that this dilatation will

be of order $1/N$ for any atom of concern to us. There-
fore, for large N the configuration of atoms close to the
defect will be given correctly by Eq. (1).

[8]J. R. Hardy and R. Bullough, Phil. Mag. 15, 237
(1967).

[9]N_{max} is determined by computer speed.

[10]J. W. Flocken, Phys. Rev. B 1, 2447 (1970).

[11]Zdendk Kopal, *Numerical Analysis* (Wiley, New York,
1955), Chap. VII; and *Handbook of Mathematical Functions*
(U. S. Department of Commerce, National Bureau of
Standards, Washington, D. C., 1964), Appl. Math. Series
55, p. 887.

[12]J. L. Yarnell, J. L. Warren, and S. H. Koenig, in
Lattice Dynamics, edited by R. F. Wallis (Pergamon,
London, 1965), p. 57.

[13]C. B. Walker, Phys. Rev. 103. 547 (1956).

[14]J. R. Hardy, J. Phys. Chem. Solids 29, 2009
(1968).

[15]The Gaussian Quadrature with n positive roots of a
function $f(x)$ over the interval -1 to 1 is exact if $f(x)$ is
a polynomial in x of degree less than $4n$. Thus, by
approximating the displacement field according to Eq.
(8), we are in effect integrating exactly an expanded form
for the integrand. In particular, the integrand is effec-
tively expanded in a Taylor series of order $4n-1$ in each
of the variables, x, y, and z, about either $+\frac{1}{2}\pi$ or $-\frac{1}{2}\pi$
depending on whether the variable is positive or negative.
As $\bar{l}$ increases, the oscillatory behavior of the integrand
becomes more pronounced until at some point the effective
expansion breaks down; and this breakdown, when it
occurs, takes place very sharply.

Kohler's Rule and the Transverse Magnetoresistance of Very Dilute *Cu*Mn, *Cu*Fe, and *Cu*Co Alloys

C. M. Hurd and J. E. A. Alderson

Division of Chemistry, National Research Council of Canada, Ottawa K1A OR9, Canada

(Received 19 April 1971)

The transverse magnetoresistance has been measured at 4.2 °K in polycrystalline alloys of
Cu containing Co, Fe, or Mn, three solutes of respectively increasing magnetism. The solute
concentrations are in the range 9–4000 at. ppm. Deviations from Kohler's rule in the low-
field condition confirm the relative anisotropies of the solute potential scattering previously ob-
tained from the Hall effect, and incidentally lead to a value of τ_B/τ_N of 0.9 for Co in Cu. The
dependence upon solute concentration of the negative magnetoresistance in the *Cu*Mn alloys
(23–271 ppm) shows an unexplained property: It is concentration independent and in agreement
with previous work for the more concentrated samples, but becomes dependent upon concen-
tration below about 70 ppm where no previous measurements exist. The importance of sample
size effects in such measurements upon very dilute alloys is illustrated.

I. INTRODUCTION

According to Kohler's rule, the galvanomagnetic
effects in a metal are functions of H/ρ_0, where H
is the applied field strength and ρ_0 is the electrical
resistivity when $H = 0$. The circumstances under
which this rule breaks down as the temperature
or purity is altered have been discussed frequently
in the literature.[1] These include cases where an
effective change in the topology of the Fermi sur-
face is produced (as, for example, by magnetic
breakdown or localized interorbital electron scat-
tering) or where the anisotropy of the average
electronic relaxation time (τ) is changed (as can
happen when two or more comparable scattering
processes of different anisotropies coexist). A
Kohler diagram can therefore frequently be a
convenient presentation for discussing the contri-
bution of these effects to the field dependence of
a given galvanomagnetic property.

It is the purpose of this paper to discuss the ap-
plication of a Kohler diagram to the isothermal
transverse magnetoresistance of very dilute alloys
of Cu containing solutes possessing varying degrees
of magnetism. Following some recent work by us[2]
showing evidence of possible solute clustering ef-
fects in such systems, we are particularly inter-
ested in their behavior as the solute's concentra-
tion is reduced to zero. The paper therefore
deals with results obtained for very dilute alloys
where the measurements inevitably encompass
the intermediate-field region, i.e., between the
low-field region ($\omega\tau \ll 1$), where the dominant
scattering process governs the behavior of the
magnetoresistance, and the high-field region
($\omega\tau \gg 1$), where only the topology of the Fermi
surface and the degree of compensation are im-
portant. (ω is here the cyclotron frequency cor-
responding to H.)

The work has involved the measurement at
4.2 °K of the transverse magnetoresistance of
polycrystalline samples of Cu containing Mn, Fe,
or Co with an approximate concentration in the
range 9–4000 at. ppm. The results lead to